



Increased brain atrophy and lesion load is associated with stronger lower alpha MEG power in multiple sclerosis patients

Jeroen Van Schependom^{a,b,c,*}, Diego Vidaurre^{d,e,1}, Lars Costers^{a,b}, Martin Sjøgård^f, Diana M. Sima^g, Dirk Smeets^g, Marie Beatrice D'hooghe^{a,h}, Miguel D'haeseleer^{a,h}, Gustavo Decoⁱ, Vincent Wens^{f,j}, Xavier De Tiège^{f,j}, Serge Goldman^{f,j}, Mark Woolrich^{d,e}, Guy Nagels^{a,b,h,k}

^a Neurology, Center for Neurosciences, Vrije Universiteit Brussel (VUB), Universitair Ziekenhuis Brussel (UZ Brussel), Laarbeeklaan 101, 1090 Brussels, Belgium

^b AIMS, Center for Neurosciences, Vrije Universiteit Brussel (VUB), Laarbeeklaan 103, 1090 Brussels, Belgium

^c Department of Electronics and Informatics (ETRO), Vrije Universiteit Brussel, Pleinlaan 2, Brussels, Belgium

^d Oxford Centre for Human Brain Activity (OHBA), University of Oxford, United Kingdom

^e Oxford University Centre for Functional MRI of the Brain (FMRIB), University of Oxford, United Kingdom

^f Laboratoire de Cartographie fonctionnelle du Cerveau, UNI-ULB Neuroscience Institute, Université libre de Bruxelles (ULB), Brussels, Belgium

^g icometrix NV, Kolonel Begaultlaan 1b / 12, 3012 Leuven, Belgium

^h National MS Center Melsbroek, 1820 Melsbroek, Belgium

ⁱ Computational Neuroscience Group, Universitat Pompeu Fabra, Spain

^j Magnetoencephalography Unit, Department of Functional Neuroimaging, Service of Nuclear Medicine, CUB-Hôpital Erasme, Brussels, Belgium

^k St Edmund Hall, University of Oxford, United Kingdom

¹ Center for Functionally Integrative Neuroscience, Department of Clinical Medicine, Aarhus University, Aarhus 8000, Denmark

ARTICLE INFO

Keywords:

Multiple sclerosis
Structural neuroimaging
Magnetoencephalography
Resting state
Spectral power

ABSTRACT

In multiple sclerosis, the interplay of neurodegeneration, demyelination and inflammation leads to changes in neurophysiological functioning. This study aims to characterize the relation between reduced brain volumes and spectral power in multiple sclerosis patients and matched healthy subjects.

During resting-state eyes closed, we collected magnetoencephalographic data in 67 multiple sclerosis patients and 47 healthy subjects, matched for age and gender. Additionally, we quantified different brain volumes through magnetic resonance imaging (MRI).

First, a principal component analysis of MRI-derived brain volumes demonstrates that atrophy can be largely described by two components: one overall degenerative component that correlates strongly with different cognitive tests, and one component that mainly captures degeneration of the cortical grey matter that strongly correlates with age. A multimodal correlation analysis indicates that increased brain atrophy and lesion load is accompanied by increased spectral power in the lower alpha (8–10 Hz) in the temporoparietal junction (TPJ). Increased lower alpha power in the TPJ was further associated with worse results on verbal and spatial working memory tests, whereas an increased lower/upper alpha power ratio was associated with slower information processing speed.

In conclusion, multiple sclerosis patients with increased brain atrophy, lesion and thalamic volumes demonstrated increased lower alpha power in the TPJ and reduced cognitive abilities.

1. Introduction

The prevalence of cognitive impairment (CI) in multiple sclerosis is estimated between 40 and 70% (Chiaravalloti & DeLuca, 2008). Whereas information processing speed is the most commonly affected

cognitive domain (Strober et al., 2009), attention, working memory and verbal fluency are also frequently affected (Langdon et al., 2012). However, assessing a patient's cognitive status is a time-demanding task. Furthermore, as there are only a limited number of standardized cognitive tests, the results are prone to practice effects (Van et al., 2014).

* Corresponding author at: Centre for Neurosciences, Vrije Universiteit Brussel, Laarbeeklaan 101, 1090 Brussels, Belgium
E-mail address: Jeroen.van.schependom@vub.be (J. Van Schependom).

<https://doi.org/10.1016/j.nicl.2021.102632>

Received 22 July 2020; Received in revised form 5 February 2021; Accepted 11 March 2021

Available online 17 March 2021

2213-1582/© 2021 The Author(s).

Published by Elsevier Inc.

This is an open access article under the CC BY-NC-ND license

(<http://creativecommons.org/licenses/by-nc-nd/4.0/>).

Therefore, a biomarker that can objectively assess a patient's cognitive status would be of great value. One candidate for such a biomarker is the quantification of the volume of different brain structures based on magnetic resonance imaging (MRI). However, although brain atrophy is a well-known feature of MS, its correlation with a patient's cognitive status is currently not sufficient (D'hooghe et al., 2019).

A potential alternative biomarker is the characterization of the brain's activity measured through electro- or magnetoencephalography (EEG/MEG) or functional MRI (fMRI). Whereas fMRI is most widely used, it captures only the slow fluctuations and may be affected by hypoperfusion (D'haeseleer et al., 2015; Zhang et al., 2019). In contrast to fMRI, EEG and MEG measure the electrical activity more directly, i.e., without convolution with the hemodynamic response function. Whereas both pick up similar sources, MEG is generally considered to have a better spatial resolution. For a more detailed comparison see (Lopes et al., 2013).

In the absence of a specific task, the brain's electrical activity can be characterized in different ways: one way is the construction of cortical networks by calculating the correspondence between time series measured at different locations (Brookes et al., 2011; Sjøgård et al., 2019). Another is the analysis of the different time series as a series of short-living transient networks (Baker et al., 2014; de Pasquale et al., 2012; O'Neill et al., 2015; Van Schependom et al., 2019; Vidaurre et al., 2016). Yet, a straightforward candidate is the power spectrum density (PSD) in different brain regions. Engemann et al recently demonstrated that adding MEG PSD substantially improved age prediction (Engemann & Combining, 2020).

Power spectral density estimates have already been successfully explored as potential biomarkers for cognitive functioning in MS. Using EEG Leocani et al. demonstrated a stronger theta power in frontoparietal regions in MS patients (Leocani et al., 2000), whereas Van Schependom et al. reported a weaker delta power in the frontoparietal regions in MS (Van Schependom et al., 2019). With relation to cognitive impairment, Keune et al recently demonstrated an association between increased global lower and upper alpha power and an increased frontal theta/beta ratio, a marker of attention control, with lower scores of information processing speed (Keune et al., 2017, 2019). Furthermore, Schoonhoven et al reported a decreased alpha peak frequency in cognitively impaired MS patients (Schoonhoven et al., 2019). Interestingly, alpha oscillations at least partially arise from thalamocortical feedback loops (Hindriks et al., 2015) and both thalamic atrophy and alpha oscillations have been consistently linked with cognitive impairment in MS (Houtchens et al., 2007; Razvan et al., 2018; Tewarie et al., 2013).

Yet, to the best of our knowledge, we are not aware of studies linking MS-induced structural damage to changes in electrophysiological spectral power as assessed through EEG or magnetoencephalography (MEG). In this paper, we quantify MRI-based volumes and the MEG power spectral density in a large cohort of MS patients and healthy subjects. Our goal is to understand how damage to the brain's structures affects brain functioning by correlating whole-brain MR markers with MEG power spectral density.

2. Methods

2.1. Patient population

From 2015 to 2018, we collected MEG data and T1- and FLAIR-weighted MR images in a cohort of 67 MS patients and 47 healthy subjects (HS), matched on age and gender. Patients with MS were recruited at the National MS Center Melsbroek (Belgium). Inclusion criteria were: diagnosis with relapsing remitting MS according to the revised McDonald criteria (Polman et al., 2011), age between 18 and 60 years old, and having an Expanded Disability Status Scale (EDSS, (Kurtzke, 1983) ≤ 6 . Exclusion criteria were a relapse or treatment with corticosteroids in the 6 weeks preceding the study, pacemaker, dental wires, concomitant psychiatric disorders (e.g., major depressive

disorder), epilepsy and benzodiazepine treatment.

2.2. MEG and MRI assessment

The MEG data was collected at the CUB Hôpital Erasme (Brussels, Belgium) on an Elekta Neuromag Vectorview scanner (Elekta Oy, Helsinki, Finland) for the first 30 multiple sclerosis patients and 15 HSs and on an Elekta Neuromag Triux scanner (MEGIN, Croton Healthcare, Helsinki, Finland) for the remaining cohort due to an upgrade in the facilities. Both MEG scanners share similar sensor layout (102 triple sensors, each consisting of one magnetometer and two orthogonal planar gradiometers) and were placed in a lightweight magnetically shielded room (Maxshield™, Elekta Oy, Helsinki, Finland). As changes with respect to signal-to-noise-ratio or sensitivity to specific frequency bands may affect results, we included the MEG scanner type as a covariate in our statistical models.

During MEG data collection, all participants were asked to close their eyes and think of nothing specifically (eyes-closed resting-state condition) for 10 min. MEG signals were recorded with a 0.1–330 Hz pass-band filter at 1 kHz sampling rate. Subjects' head position inside the MEG helmet was continuously monitored using four head-tracking coils. The location of these coils and at least 400 head-surface points (on the nose, face, and scalp) with respect to anatomical fiducials were determined with an electromagnetic tracker (Fastrak, Polhemus, Colchester, Vermont, USA). Simultaneous with the MEG signal acquisition, an electrooculogram (EOG) and electrocardiogram (ECG) were recorded.

MRI was performed on a 3 T Achieva scanner (Philips Medical Systems, Best, The Netherlands). The scanner protocol contained a 3D T1-weighted sequence (TR: 4.939 ms, FA 8°, 230x230 mm² FOV, 310 sagittal slices; resulting in a 0.53 by 0.53 by 0.5 mm³ resolution) and a FLAIR (TR = 4800 ms, TE = 316 ms, TI = 1650 ms, 321 frames, field of view = 288 × 288 mm, slice thickness = 1.12 mm).

The median delay between the MRI and MEG session across all subjects was 5 days with an interquartile range of 2–10 days.

2.3. MEG processing

MEG data were first preprocessed offline with the temporal extension of the signal space separation algorithm (Maxfilter™, Elekta Oy, Helsinki, Finland, version 2.2 with default parameters) to subtract external interferences and correct for head movements (Taulu et al., 2005). Movement parameters were stored for later analysis.

All data were then downsampled to 250 Hz, automatically coregistered with the subject's T1 image using RHINO, OSL's (<https://github.com/OHBA-analysis>) algorithm to coregister head shape points to the scalp extracted using FSL's BETSURF and FLIRT (Jenkinson et al., 2002; Smith, 2002), and transformed in a common MNI152-space (Mazziotta et al., 1995). Data were filtered between 1 and 70 Hz with an additional notch filter (48–52 Hz). Additionally, we added a notch filter with center frequency at 16.6 Hz as we noticed a strong peak in spectral power at this frequency. This artefact is likely due to mechanical vibrations induced by construction works at the hospital site at the time of acquisition. After a visual check to remove artefactual time segments, an independent component analysis (ICA) was run to exclude ocular and cardiac artefacts based on the correlation of the components' time course with ECG and EOG. After filtering into the frequency band of interest (1–46 Hz), source reconstruction was performed using a linearly constrained minimum variance beamformer to an 8 mm cortical grid using a local spheres head model generated through FieldTrip (Oostenveld et al., 2011; Quinn et al., 2018; Woolrich et al., 2011).

2.4. Parcellation

Next, the cortex was parceled using a custom parcellation atlas consisting of 42 parcels: 38 parcels were based on an ICA of fMRI data from the Human Connectome Project, the remaining four parcels

correspond to the anterior and posterior precuneus and left and right intraparietal sulci as discussed before (Van Schependom et al., 2019; Vidaurre et al., 2018). The parcellation atlas spanned the complete cortex and did not include subcortical areas. For each parcel, the first principal component (PC) of the different timeseries within that parcel was used as that parcel's time series.

2.5. Power spectral density

For each parcel, the power spectral density was calculated using MATLAB's standard `pwelch` function with a window length of 1024 samples (4 s). Before entering statistical analyses, spectra were normalized by dividing through their L1-norm. For descriptive purposes, we define global spectral power as the averaged spectral power density across all parcels.

2.6. MRI processing & segmentation

The **icobrain** pipeline (version 3.1) segments a T1-weighted image into white matter, grey matter and cerebrospinal fluid. White matter FLAIR hyper-intensities are identified and included in the white matter segmentation. The main blocks of the **icobrain** pipeline have been described previously (Jain et al., 2015); in short, after skull stripping and bias correction, the T1 weighted image is segmented using a probabilistic image intensity model and non-rigidly propagated tissue priors from an MNI atlas (Mazziotta et al., 1995). Lesion segmentation is obtained by iterating the following loop until convergence: segmentation of the T1-weighted image, identification of intensity outliers on the FLAIR image and filling of the lesions on the T1-weighted image (Jain et al., 2015; Smeets et al., 2016). T1 hypointensities, also called black holes, are also obtained as a sub-segmentation of the FLAIR lesions. Importantly, there is some debate on the sensitivity of 3D-T1 sequences in detecting T1 hypointensities. Typically, a 3D sequence detects more but less severe hypointensities (Lapucci et al., 2020). **icobrain** further refines the main tissue segmentation in order to obtain sub-segmentations of cortical grey matter and thalami (Cardoso et al., 2013). Brain volumes (except for lesion load and black holes volume) are normalized for head size. In summary, the **icobrain** pipeline thus leads to the quantification of the whole brain white matter, deep and cortical grey matter, lesion load and black hole and thalamic volumes.

2.7. Neuropsychological assessment

At the day of the MEG assessment, all subjects underwent neuropsychological testing. The neuropsychological tests included the Symbol Digit Modalities Test (SDMT), a test designed to capture information processing speed, the Dutch version of the California Verbal Learning Test (CVLT-II) to assess verbal memory, the Controlled Oral Word Association Test (COWAT) to assess verbal fluency and the Brief Visuospatial Memory Test (Revised; BVM-T-R) to assess spatial memory. More details can be found in (Costers et al., 2017; Van Schependom et al., 2014). Fatigue was assessed through the Fatigue Scale for Motor and Cognitive Functions (Penner et al., 2009).

2.8. Uni- and multimodal analyses

As different brain volumes can be expected to be strongly correlated, we performed a principal component analysis (PCA) on the MR derived whole brain volumes of the full cohort to allow the extraction of those components that explain most variance. This results in as many principal components as PCA input variables (in our case: 5), but with the advantage that we can limit the analysis to those components that explain a large portion of the variance instead of having to repeat the same analysis for different correlated variables. Finally, we correlated the spectral power with the PC weights obtained for each subject in order to assess the correlation between brain damage and oscillatory

power.

2.9. Statistics

Covariations within and between modalities have been assessed through the Pearson correlation coefficient. All analyses have been performed within the general linear model and continuous covariates were first z-transformed before being included in the design matrix. All reported results have been corrected for age, gender, scanner and education by including them as covariates of no interest in the model design.

All presented p-values were obtained by creating a null-distribution of the statistic of interest through 5000 permutations. For each permutation, each frequency bin and each parcel, we thus obtained a value of the t-statistic. Next, we calculated the threshold-free cluster enhancement (TFCE) across frequencies and created a null distribution of maximum TFCE values across parcels and frequency bins. Finally, the actual TFCE t-statistics were compared to this null distribution and all TFCE t-statistics above the 97.5th or below the 2.5th percentile were considered significant, equivalent with a cutoff p-value of 0.05. The use of TFCE allows us to assess whether specific frequency bands of interest emerge without us imposing traditional bands. Further it does not require the definition of a predefined threshold to detect clusters (SMITH & NICHOLS, 2009). For the multimodal analyses presented in this paper, we will report TFCE corrected p-values defined as the percentile within this null distribution.

2.10. Ethics

All subjects provided written informed consent and the study was approved by the local ethics committees of the University Hospital Brussels (Commissie Medische Ethiek UZ Brussel, B.U.N. 143201423263, 2015/11) and the National MS Center Melsbroek (2015-02-12).

3. Results

3.1. Patient population

We provide a detailed description of the included cohorts of MS patients and HSs and basic MRI and MEG results in Table 1. As expected, all MR-derived brain volumes significantly differ between the MS and HS population despite both populations being matched for age and gender with only a minor difference in education ($p = 0.03$, uncorrected). No differences could be observed between the two cohorts for what concerns global MEG spectral power although upper alpha power shows a trend to be stronger in the HSs ($p = 0.05$, uncorrected). Finally, the MS cohort performs worse on all cognitive tests.

3.2. Principal component analysis of MRI parameters

In Fig. 1, we present the results of the PCA on the MR parameters across all subjects. The first PC explains about 55% of the variance and indicates a covarying pattern of smaller white and grey matter with larger volumes of white matter lesion volume and black holes. The second PC mainly picks up variations in cortical grey matter and explains 19.2% of variance. Subsequent PCs explain at most 10% of the variance.

As a PCA is only determined up to the sign, it is important to clarify the meaning. The first PC has negative weights in the HS population (mean: -1.2) as compared to positive weights in the MS population (mean: 0.68). This essentially means that a strong negative weight of this component relates to more (C)GM, WM and a smaller lesion volume than the average subject. Similarly, the second PC correlates strongly with age (both across the full cohort as within the two subcohorts) and has positive weights in young healthy subjects and negative weights in older healthy subjects. This indicates that a higher score on PC2 relates to

Table 1

Cohort characterisation. We report the mean values and standard deviations from the different clinical, structural and functional parameters for both the MS and healthy cohort. For EDSS the median and interquartile range (IQR) is shown. The comparisons were performed using permutation testing with $N = 5000$ for all parameters except gender and onset type for which a chi-squared test was used. All reported MRI based volumes have been normalized for head size.

	Healthy subjects (HS)	MS patients	HS vs MS
N	46	66	–
Gender (M/F)	18/28	28/38	0.71
Age (yrs)	47 (12)	49 (10)	0.52
Disease duration (yrs)	–	16.5 (9)	–
EDSS median [IQR]	–	2.5 [2–3]	–
Relapsing remitting vs secondary progressive	–	62/4	–
Education (Yrs)	15 (2)	14 (3)	0.03
MRI			
White matter volume (ml)	640 (41)	607 (42)	<0.001
Cortical grey matter volume (ml)	854 (55)	829 (46)	0.01
Deep grey matter volume (ml)	44 (4.1)	40 (4.7)	<0.001
Lesion load (ml)	1.9 (1.8)	9.6 (8.0)	<0.001
Black holes (ml)	1.1 (1.2)	6.3 (5.6)	<0.001
Thalamus (ml)	13.2 (1.2)	11.6 (1.4)	<0.001
Global MEG spectral power			
Delta (1–4 Hz)	0.18 (0.03)	0.18 (0.04)	0.84
Theta (4–8 Hz)	0.18 (0.03)	0.19 (0.05)	0.29
Lower alpha (8–10 Hz)	0.14 (0.04)	0.015 (0.05)	0.13
Upper alpha (10–12 Hz)	0.14 (0.04)	0.13 (0.04)	0.05
Beta (12–30 Hz)	0.37 (0.06)	0.36 (0.07)	0.52
Gamma (30–40 Hz)	0.04 (0.01)	0.04 (0.01)	0.99
Cognitive test results			
Symbol Digit Modalities Test	54 (9.6)	48 (12)	0.009
California Verbal Learning Test II	65 (7.1)	61 (11.2)	0.029
Controlled Oral Word Association Test	11.1 (3.8)	8.8 (3.1)	0.001
Brief Visuospatial Memory Test - Revised	28.7 (5.3)	25.1 (6.9)	0.002

more (cortical) grey matter and lower age than the average subject.

Comparing the PC weights between both cohorts shows that only the first component significantly differs between MS and HSs ($p = 1E-8.6$). When repeating the PCA for both subcohorts independently, PC1 emerges in both cohorts (see Figs. A1 and A2).

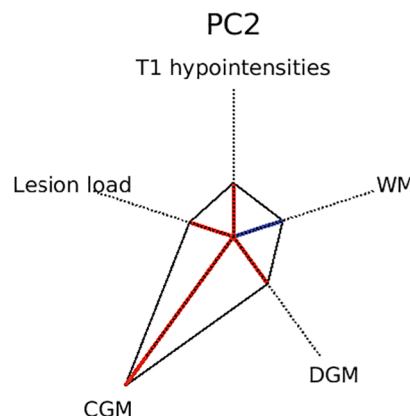
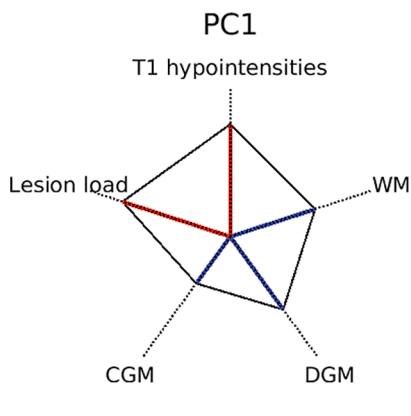


Fig. 1. Principal component analysis of the MR derived brain volumes. Illustration of the two principal components revealed by the MR derived brain volumes from all subjects. PC1 is a linear combination that receives positive contributions from lesion and black hole volumes (red) and negative contributions from the white, deep and cortical grey matter (blue). PC2 is specific to cortical grey matter. (For interpretation of the references to colour in this figure legend, the reader is referred to the web version of this article.)

3.3. Correlation between MRI parameters and cognitive impairment

The first PC correlates with thalamic volume ($r = -0.83$, $p < 0.001$) and different cognitive tests: information processing speed (SDMT, $r = -0.44$, $p < 0.001$), verbal learning and memory (CVLT-II, $r = -0.42$, $p < 0.001$) and spatial memory (BVM-T-R, $r = -0.31$, $p < 0.001$). Similarly, thalamic volume correlates with SDMT ($r = 0.39$, $p < 0.001$), CVLT-II ($r = 0.4$, $p < 0.001$) and BVM-T-R ($r = 0.3$, $p < 0.001$). The second PC correlates strongly with age ($r = -0.53$, $p < 0.001$), but not with any other clinical test. The remaining PCs are not significantly correlated with any clinical covariate. As ageing is not the focus of this paper, we only include PC1 in further analyses. All mentioned correlations are calculated across the full cohort.

3.4. Multimodal structure–function correlations

After correction across frequency bins and parcels, PC1 was shown to be negatively correlated with spectral power between 8 and 9 Hz in the temporoparietal junction (TPJ). Fig. 2 shows, on the left-hand side, the p-value of these negative correlations and on the right-hand side a scatter plot of PC-weights vs spectral power for both cohorts. Similarly, we show a negative correlation between thalamic volumes and spectral power in the same frequency with a similar spatial profile.

As indicated in Fig. 2, the correlations between spectral power and PC1 are only significant in the MS cohort and not in the HS. The same goes for the correlation between alpha power and thalamic volume. This is likely caused by a broader range in PC1 weights and thalamic volumes in the MS patients. Correlations with individual MR parameters included in the PCA are shown in Fig. A3 (white matter volume, lesion load, and black holes). Correlations between spectral power and PC1 on a voxel-level (instead of the parcellation approach) are shown in Fig. A4.

3.5. Increased lower alpha power in MS cohort with increased atrophy and lesion load

In order to further investigate the correlation between higher levels of MS related neurodegeneration and stronger lower alpha power, we split the MS cohort on the median of the PC1 weights, creating a group with above average PC1 weights (ie above average brain atrophy and lesion load) and a group with below average PC1 weights (i.e. below average brain atrophy and lesion load). These MS subgroups did not differ on gender ($p = 0.12$, Chi2 test) nor on education, age or COWAT ($p > 0.05$), but did differ on SDMT ($p = 0.002$), CVLT-II ($p < 0.001$) and BVM-T-R ($p = 0.01$) as expected from the previously presented correlations between PC1 and cognition. Further, we observed a significant increase in lower alpha power ($p = 0.007$) in the more affected group. This group also displayed higher EDSS scores ($p = 0.02$). We plot the spectra in the left TPJ in Fig. 3.

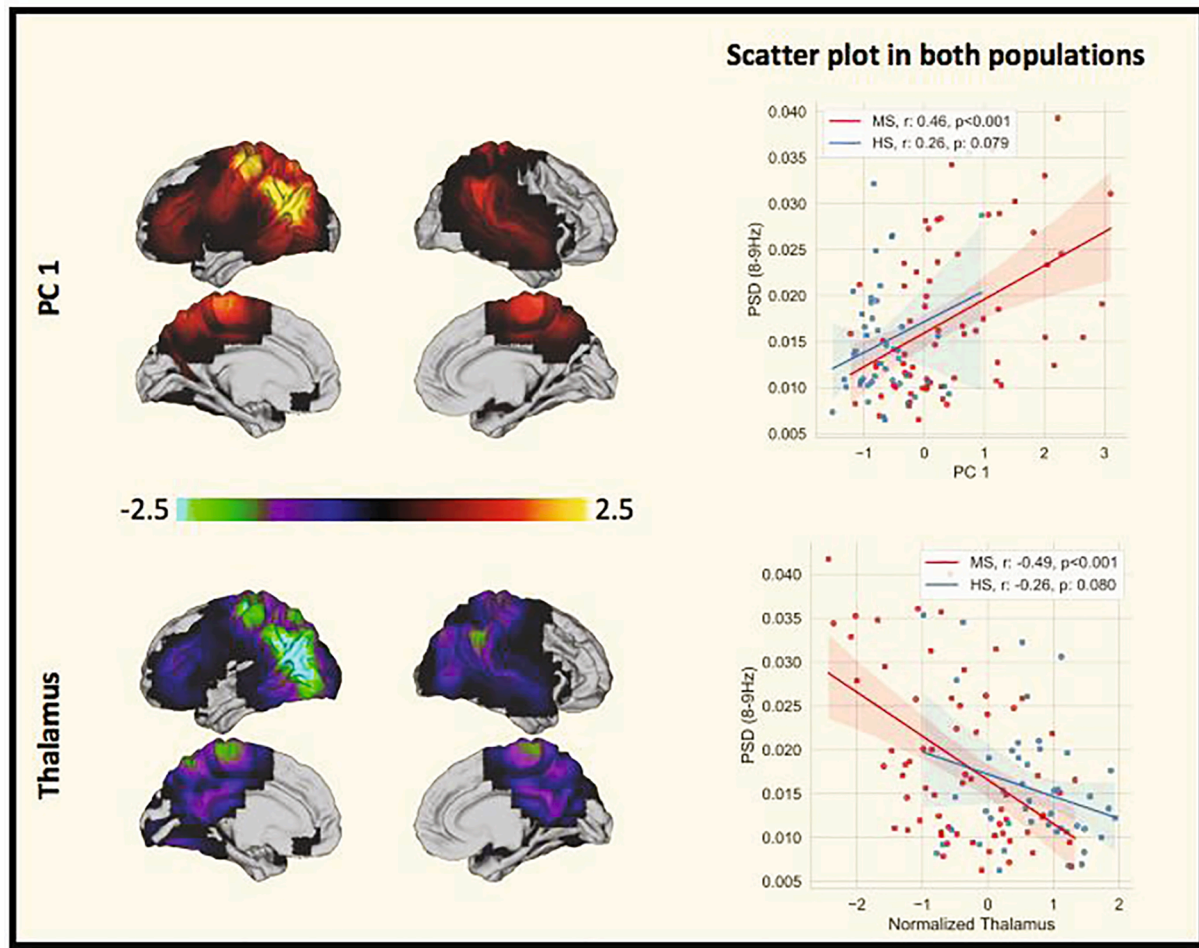


Fig. 2. Multimodal correlations. Left: $-\log_{10}$ of the p-value of the correlations between PC1 (upper panel) or Thalamic volume (lower panel) and MEG spectral power in the MS cohort after correction across parcels and frequency bins; the colour indicates the strength of significance and the sign the direction of the effect (+ = positive, - = negative). Right: scatter plots between spectral power in the temporoparietal junction (TPJ) and PC1-weights (upper panel) or thalamic volume (lower panel) for both cohorts. The subtitles indicate for each cohort the Pearson correlation and its corresponding p-value. PSD = Power Spectral Density.

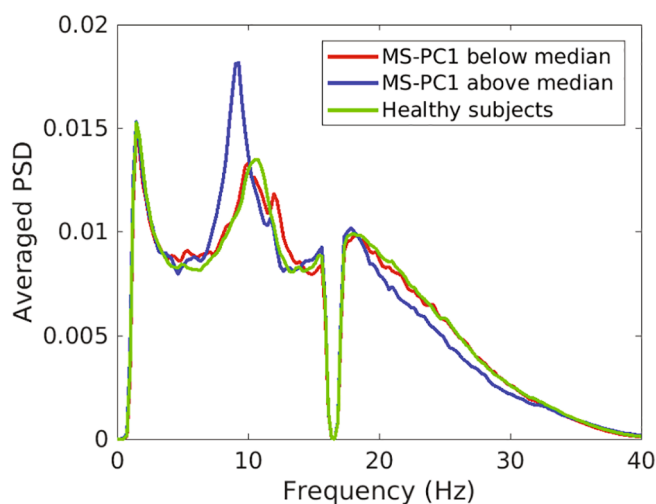


Fig. 3. Relative spectral power in three groups in the temporoparietal junction: the MS cohort was split on the median of MS-related degeneration: the blue curve indicates MS patients with stronger brain atrophy and higher lesion load. The red curve those with less brain atrophy and lesion load and green is the PSD of the healthy subjects. The dip at 16.6 Hz results from the notch filter as explained in the methodology. (For interpretation of the references to colour in this figure legend, the reader is referred to the web version of this article.)

When splitting on the median of thalamic volume, the group with smaller thalamic volumes trended towards higher EDSS scores ($p = 0.06$) and worse SDMT ($p = 0.06$), performed significantly worse on CVLT-II ($p = 0.009$), but not on COWAT ($p = 0.47$) nor spatial memory ($p = 0.45$). A similar plot to Fig. 3 is obtained when splitting on thalamic volume. All reported p-values are obtained through permutation testing ($N = 5000$).

3.6. Correlation between alpha power and cognitive functioning

In order to simplify the comparison with the literature using, we will refer to our results in the 8–9 Hz band as “lower alpha band” as it is contained in the traditionally defined lower alpha band (see e.g. Tewarie et al., 2013). Given the strong correlation between PC1 weights and cognition on the one hand and the strong correlations between PC1 weights and lower alpha power in the TPJ on the other, we also assessed the correlation between alpha power in the TPJ and cognition directly. Lower alpha power of the TPJ correlates with CVLT-II ($r = -0.31$, $p < 0.001$) and BVMT-R ($r = -0.27$, $p = 0.002$). There is no correlation between lower alpha power and SDMT or COWAT, but there is a correlation between SDMT and upper alpha power ($r = 0.17$, $p = 0.048$). Consequently, there is a significant correlation between the ratio of lower and upper alpha power and SDMT ($r = -0.24$, $p = 0.005$). All correlations were calculated on the full cohort.

3.7. Correlation between alpha peak frequency and cognitive functioning

Finally, we determined the peak frequency and amplitude as the maximal frequency in the 7–14 Hz window. While we did not observe a difference between the two MS sub cohorts, we did observe a correlation between peak frequency of the TPJ with BVMT-R ($r = 0.19$, $p = 0.03$) and CVLT-II ($r = 0.22$, $p = 0.01$).

4. Discussion

In this paper we provide a novel multimodal analysis of how MS concurrently affects brain structure and functioning. First, we demonstrate that a large portion of intersubject variance in MR parameters can be explained by two principal components. Whereas the first PC picks up atrophy and lesion load, and is strongly correlated with cognitive outcomes, the second PC picks up variations mainly in the cortical grey matter and correlates strongly with age.

Furthermore, we demonstrate a strong correlation between lower alpha power in the TPJ and brain atrophy and lesion load. Without a priori assumptions, our results justify the division of the traditional alpha band in a lower and upper alpha band although the lower alpha band (8–9 Hz) slightly differs from the traditional 8–10 Hz as used in different previous studies. A decrease in upper alpha and increase in lower alpha band was previously shown in MS patients (Van der Meer et al., 2013). Here we show that this relation is associated with brain atrophy and lesion load and that this relation is most strongly expressed in the TPJ.

While our unimodal MRI analysis has some similarities with the PCA of cortical atrophy as presented by Steenwijk et al. (Steenwijk et al., 2016), there are important differences. In this study, we performed a PCA on different brain volumes instead of cortical thickness patterns. This precludes us from discussing where precisely in the brain the atrophy occurs but allows us to include different MR derived brain volumes in the PCA (e.g., lesion load, ...) to capture different disease processes. As we are studying a patient population with an average disease duration of 16.5 years, most patients' brains will be substantially affected by both demyelination and neurodegeneration and both aspects cannot be disentangled.

The strongest correlation between measures of whole-brain damage and local oscillatory power is found in the TPJ. Interestingly, the TPJ is strongly connected to the thalamus (Kucyi et al., 2012), which in itself is one of the first regions affected by neurodegeneration in MS (Razvan et al., 2018, 2018) and its atrophy showed a similar correlation with lower alpha power in this cohort. Importantly, PC1 significantly correlated with cognitive tests assessing information processing speed (IPS), verbal and spatial learning abilities.

The left TPJ contains the left angular gyrus (LAG) which has recently emerged as a major hub involved in different cognitive tasks (Seghier, 2013) and is part of the default mode network (DMN). The importance of an intact DMN for information processing speed (IPS) is emphasized by (Savini et al., 2019) who reported a significant correlation between DMN global efficiency and IPS in relapsing onset MS patients. As the AG is involved in different cognitive tasks, an increase in lower alpha power could indicate an increase in inhibition and reduced cognitive abilities (Haegens et al., 2011).

In order to understand this correlation better, we performed a post-hoc analysis and divided the MS cohort based on the median of the MS-specific structural damage. This analysis suggests that the increase in lower alpha power is induced by both a slowing of the alpha-peak frequency and an increase of the alpha-peak power. This corresponds to the reduced peak frequency in the TPJ in cognitively impaired MS patients as reported in (Schoonhoven et al., 2019). Of note, a reduced peak frequency has also been observed in Alzheimer's disease (Goossens et al., 2016).

While we observe correlations between lower alpha power in the TPJ and tests of verbal and spatial memory, we do not observe the negative

correlations between lower and upper alpha power and SDMT as observed in (Keune et al., 2017; Van der Meer et al., 2013). Yet there are also differences in study design: Keune et al used EEG and a combination of eyes closed and eyes open paradigms with a relatively coarse frequency resolution of 1 Hz (as compared to 0.25 Hz in this paper) and Van Der Meer et al used global relative power and a composite measure of different neuropsychological tests.

The alpha peak frequency has been demonstrated to vary both within and across subjects with standard deviations being 0.9 and 2.8 Hz respectively (Haegens et al., 2014). The observed group-level difference in alpha peak frequency (1.5 Hz) is larger than the previously reported intrasubject variation (Haegens et al., 2014). Interestingly, Benwell and colleagues reported an increase in alpha power and slowing of the alpha peak frequency (at a rate of 0.2 Hz/hour) during a trial (Benwell et al., 2019). An increase in alpha-power has previously been associated with decreases in sustained attention and increased fatigue (see e.g. (Cajochen et al., 1995)). Yet, splitting the data on the median FSMC score - a measure of fatigue - did not reveal a difference in spectral power.

It is important to bear in mind that this study did not make any assumptions on which frequency bin could be affected by MS and our results thus highlight the alpha band as the frequency band of interest. Future research should investigate whether alpha-power and peak frequency are consistently higher (resp. lower) in MS patients with impaired cognition or that their alpha-power and peak-frequency drift more during the recording.

The main strength of this study is that we explored the relationship between structure and function without using predefined frequency bands. Yet, we still assume a specific frequency has the same function across subjects. As our results with individual MR parameters indicate, the individual contributions of MR damage to local changes in oscillatory power are difficult to disentangle, but the strongest correlations are observed between white matter or thalamic volume and alpha power, suggesting a disruption of the thalamocortical circuitry. Another important limitation of resting-state eyes closed is that the results may be affected by different cohorts being more likely to fall asleep. We consider this unlikely to affect our results as falling asleep would induce an increase in theta power and decrease in alpha power, which was not observed. Furthermore, we redid the analysis including only the first two minutes of data and observed similar results.

5. Conclusion

Multiple sclerosis is characterized by brain atrophy and lesion load. Yet how this structural damage leads to neurophysiological changes is only poorly understood. In this article, we characterized this structure-function relationship as a first step towards understanding how structural damage affects functioning. We demonstrated that MS patients with more brain atrophy and a higher lesion load displayed increased lower alpha power in the TPJ and impaired cognitive functioning and that this increase may be due to a slowing of the alpha peak frequency.

6. Data availability

Data availability requests to access the datasets generated for the current study will be considered in relation to the consents, relevant rules and regulations, and can be made via the corresponding author.

CRedit authorship contribution statement

Jeroen Van Schependom: Conceptualization, Investigation, Methodology, Software, Formal analysis, Data curation, Writing - original draft, Funding acquisition. **Diego Vidaurre:** Methodology, Writing - review & editing. **Lars Costers:** Investigation, Writing - review & editing. **Martin Sjøgård:** Investigation, Writing - review & editing. **Diana M. Sima:** Methodology, Writing - review & editing. **Dirk Smeets:**

Methodology, Writing - review & editing. **Marie Beatrice D'hooghe:** Conceptualization, Writing - review & editing. **Miguel D'haeseleer:** Conceptualization, Writing - review & editing. **Gustavo Deco:** Methodology, Writing - review & editing. **Vincent Wens:** Methodology, Writing - review & editing. **Xavier De Tiège:** Methodology, Writing - review & editing. **Serge Goldman:** Writing - review & editing. **Mark Woolrich:** Methodology, Writing - review & editing. **Guy Nagels:** Supervision, Project administration, Conceptualization, Funding acquisition.

Declaration of Competing Interest

The authors declare that they have no known competing financial interests or personal relationships that could have appeared to influence the work reported in this paper.

Acknowledgements

We would like to thank all participants (healthy controls and people with multiple sclerosis) for their time and enthusiasm to participate, Ann Van Remoortel for her help in the recruitment and Jeroen Gielen and Jorne Laton for their help in the data collection.

Funding

JVS is funded by an FWO post-doc grant (12I1817N, www.fwo.be). LC is funded by an FWO aspirant grant (11B7218N) and GN is supported by an FWO “Fundamenteel klinisch mandaat” (1805620 N). Martin Sjøgård was supported by the Wiener-Anspach Foundation (Brussels, Belgium and Oxford, UK) and is supported by the “Marc Errens” Research Convention of the Fonds Erasme (Fonds Erasme, Brussels, Belgium). Xavier De Tiège is Postdoctorate Clinical Master Specialist at the Fonds de la Recherche Scientifique (FRS-FNRS, Brussels, Belgium). Data collection was enabled by a grant provided by the Belgian Charcot foundation awarded on Jan 16, 2015, by an FWO “Krediet aan Navorser” grant (1501218 N, www.fwo.be) granted to JVS, by an unrestricted researcher initiated grant provided by Genzyme-Sanofi to GN, and by the “Marc Errens” Research Convention of the Fonds Erasme (Fonds Erasme, Brussels, Belgium). The MEG project at the CUB – Hôpital Erasme is financially supported by the Fonds Erasme pour la Recherche Médicale (Research Convention “Les Voies du Savoir”, Brussels, Belgium). DV is supported by a Novonordisk Hallas-Møller Emerging Investigator Award (0054895), and a Horizon 2020 ERC Starting Grant (850404). The publication was supported by the Belgian University Foundation (Universitaire Stichting).

Appendix A. Supplementary data

Supplementary data to this article can be found online at <https://doi.org/10.1016/j.nicl.2021.102632>.

References

- Baker, A.P., Brookes, M.J., Rezek, I.A., et al., 2014. Fast transient networks in spontaneous human brain activity. *Elife* 3, e01867.
- Benwell, C.S.Y., London, R.E., Tagliafue, C.F., Veniero, D., Gross, J., Keitel, C., Thut, G., 2019. Frequency and power of human alpha oscillations drift systematically with time-on-task. *Neuroimage*. 192, 101–114.
- Brookes, M.J., Woolrich, M., Luckhoo, H., Price, D., Hale, J.R., Stephenson, M.C., Barnes, G.R., Smith, S.M., Morris, P.G., 2011. Investigating the electrophysiological basis of resting state networks using magnetoencephalography. *Proc. Natl. Acad. Sci.* 108 (40), 16783–16788.
- Cajochen, C., Brunner, D.P., Krauchi, K., Graw, P., Wirz-Justice, A., 1995. Power density in theta/alpha frequencies of the waking EEG progressively increases during sustained wakefulness. *Sleep*. 18 (10), 890–894.
- Cardoso, J.M., Leung, K., Modat, M., et al., 2013. STEPS: Similarity and Truth Estimation for Propagated Segmentations and its application to hippocampal segmentation and brain parcellation. *Med. Image Anal.* 17 (6), 671–684.
- Chiavarallotti, N.D., DeLuca, J., 2008. Cognitive impairment in multiple sclerosis. *Lancet Neurol.* 7 (12), 1139–1151.

- Costers, L., Gielen, J., Eelen, P.L., et al., 2017. Does including the full CVLT-II and BVMTR improve BICAMS? Evidence from a Belgian (Dutch) validation study. *Mult. Scler. Relat. Disord.* 18, 33–40.
- D'hooghe, M.B., Gielen, J., Van Remoortel, A., et al., 2019. Single MRI-Based Volumetric Assessment in Clinical Practice Is Associated With MS-Related Disability. *J. Magn. Reson. Imaging*. 49 (5), 1312–1321.
- de Pasquale, F., Della Penna, S., Snyder, A.Z., Marzetti, L., Pizzella, V., Romani, G.L., Corbetta, M., 2012. A Cortical Core for Dynamic Integration of Functional Networks in the Resting Human Brain. *Neuron*. 74 (4), 753–764.
- D'haeseleer, M., Hostenbach, S., Peeters, I., Sankari, S.E., Nagels, G., De Keyser, J., D'hooghe, M.B., 2015. Cerebral hypoperfusion: A new pathophysiological concept in multiple sclerosis? *J. Cereb. Blood Flow Metab.* 35 (9), 1406–1410.
- Engemann, D.A., Kozynets, O., Sabbagh, D., et al., 2020. Combining magnetoencephalography with magnetic resonance imaging enhances learning of surrogate-biomarkers. *Elife* 9, e54055.
- Eshaghi A, Marinescu R V., Young AL, et al. Progression of regional grey matter atrophy in multiple sclerosis. *Brain*. 2018; 141(6):1665–1677.
- Goossens, J., Laton, J., Van Schependom, J., Gielen, J., Struyfs, H., Van Mossevelde, S., Van den Bossche, T., Goeman, J., De Deyn, P.P., Sieben, A., Martin, J.-J., Van Broeckhoven, C., van der Zee, J., Engelborghs, S., Nagels, G., 2016. EEG dominant frequency peak differentiates between Alzheimer's disease and frontotemporal lobar degeneration. *J. Alzheimer's Dis.* 55 (1), 53–58.
- Haegens, S., Cousijn, H., Wallis, G., Harrison, P.J., Nobre, A.C., 2014. Inter- and intra-individual variability in alpha peak frequency. *Neuroimage*. 92, 46–55.
- Haegens, S., Nächer, V., Luna, R., Romo, R., Jensen, O., 2011. α -Oscillations in the monkey sensorimotor network influence discrimination performance by rhythmical inhibition of neuronal spiking. *Proc. Natl. Acad. Sci. U. S. A.* 108 (48), 19377–19382.
- Hindriks, R., Woolrich, M., Luckhoo, H., Joansson, M., Mohseni, H., Kringelbach, M.L., Deco, G., 2015. Role of white-matter pathways in coordinating alpha oscillations in resting visual cortex. *Neuroimage*. 106, 328–339.
- Houtchens, M.K., Benedict, R.H.B., Killiany, R., Sharma, J., Jaisani, Z., Singh, B., Weinstock-Guttman, B., Guttmann, C.R.G., Bakshi, R., 2007. Thalamic atrophy and cognition in multiple sclerosis. *Neurology*. 69 (12), 1213–1223.
- Jain, S., Sima, D.M., Ribbens, A., et al., 2015. Automatic segmentation and volumetry of multiple sclerosis brain lesions from MR images. *NeuroImage Clin* 8, 367–375.
- Jenkinson, M., Pechaud, M., Smith, S., 2002. BET2-MR-Based Estimation of Brain, Skull and Scalp Surfaces. *Hum. Brain Mapp.* 17 (2), 143–155.
- Keune, P.M., Hansen, S., Weber, E., Zapf, F., Habich, J., Muenssinger, J., Wolf, S., Schönenberg, M., Oschmann, P., 2017. Exploring resting-state EEG brain oscillatory activity in relation to cognitive functioning in multiple sclerosis. *Clin. Neurophysiol.* 128 (9), 1746–1754.
- Keune, P.M., Hansen, S., Sauder, T., Jaruszowicz, S., Kehm, C., Keune, J., Weber, E., Schönenberg, M., Oschmann, P., 2019. Frontal brain activity and cognitive processing speed in multiple sclerosis: An exploration of EEG neurofeedback training. *NeuroImage Clin.* 22, 101716. <https://doi.org/10.1016/j.nicl.2019.101716>.
- Kuciy A, Moayed M, Weissman-Fogel I, Hodaie M, Davis KD. 2012. Hemispheric asymmetry in white matter connectivity of the temporoparietal junction with the insula and prefrontal cortex. *PLoS One* 7(4).
- Kurtzke, J.F., 1983. Rating neurologic impairment in multiple sclerosis: An expanded disability status scale (EDSS). *Neurology*. 33 (11), 1444–1452.
- Langdon, D.W., Amato, M.P., Boringa, J., et al., 2012. Recommendations for a Brief International Cognitive Assessment for Multiple Sclerosis (BICAMS). *Mult. Scler. J.* 18 (6), 891–898.
- Lapucci, C., Romano, N., Schiavi, S., et al., 2020. Degree of microstructural changes within T1-SE versus T1-GE hypointense lesions in multiple sclerosis: relevance for the definition of “black holes”. *Eur. Radiol.* 30 (7), 3843–3851.
- Leocani, L., Locatelli, T., Martinelli, V., et al., 2000. Electroencephalographic coherence analysis in multiple sclerosis: correlation with clinical, neuropsychological, and MRI findings. *J. Neurol. Neurosurg. Psychiatry*. 69 (2), 192–198.
- Lopes, F., da Silva, 2013. EEG and MEG: Relevance to neuroscience. *Neuron* 80 (5), 1112–1128.
- Mazziotta, J.C., Toga, A.W., Evans, A., Fox, P., Lancaster, J., 1995. A probabilistic atlas of the human brain: theory and rationale for its development. *Neuroimage*. 2 (2), 89–101.
- O'Neill, G.C., Bauer, M., Woolrich, M.W., Morris, P.G., Barnes, G.R., Brookes, M.J., 2015. Dynamic recruitment of resting state sub-networks. *Neuroimage*. 115, 85–95.
- Oostenveld, R., Fries, P., Maris, E., Schoffelen, J.-M., 2011. FieldTrip: Open source software for advanced analysis of MEG, EEG, and invasive electrophysiological data. *Comput. Intell. Neurosci.* 2011, 1–9.
- Penner, I.K., Raselli, C., Stöcklin, M., et al., 2009. The Fatigue Scale for Motor and Cognitive Functions (FSMC): validation of a new instrument to assess multiple sclerosis-related fatigue. *Mult. Scler. J.* 15 (12), 1509–1517.
- Polman, C.H., Reingold, S.C., Banwell, B., et al., 2011. Diagnostic criteria for multiple sclerosis: 2010 revisions to the McDonald criteria. *Ann. Neurol.* 69 (2), 292–302.
- Quinn, A.J., Vidaurre, D., Abeysuriya, R., Becker, R., Nobre, A.C., Woolrich, M.W., 2018. Task-Evoked Dynamic Network Analysis Through Hidden Markov Modeling. *Front. Neurosci.* 12 <https://doi.org/10.3389/fnins.2018.00603>.
- Savini, G., Pardini, M., Castellazzi, G., et al., 2019. Default mode network structural integrity and cerebellar connectivity predict information processing speed deficit in multiple sclerosis. *Front. Cell. Neurosci.* 13, 21.
- Schoonhoven, D.N., Fraschini, M., Tawarie, P., et al., 2019. Resting-state MEG measurement of functional activation as a biomarker for cognitive decline in MS. *Mult. Scler. J.* 25 (14), 1896–1906.
- Seghier, M.L., 2013. The angular gyrus: Multiple functions and multiple subdivisions. *Neuroscientist*. 19 (1), 43–61.

- Sjögård, M., De Tiège, X., Mary, A., Peigneux, P., Goldman, S., Nagels, G., van Schependom, J., Quinn, A.J., Woolrich, M.W., Wens, V., 2019. Do the posterior midline cortices belong to the electrophysiological default-mode network? *Neuroimage*. 200, 221–230.
- Smeets, D., Ribbens, A., Sima, D.M., et al., 2016. Reliable measurements of brain atrophy in individual patients with multiple sclerosis. *Brain Behav* 6 (9), e00518.
- Smith, S.M., 2002. Fast robust automated brain extraction. *Hum. Brain Mapp.* 17 (3), 143–155.
- Smith, S., Nichols, T., 2009. Threshold-free cluster enhancement: Addressing problems of smoothing, threshold dependence and localisation in cluster inference. *Neuroimage* 44 (1), 83–98.
- Steenwijk, M.D., Geurts, J.J.G., Daams, M., et al., 2016. Cortical atrophy patterns in multiple sclerosis are non-random and clinically relevant. *Brain* 139 (Pt 1), 115–126.
- Strober, L., Englert, J., Munschauer, F., et al., 2009. Sensitivity of conventional memory tests in multiple sclerosis: comparing the Rao Brief Repeatable Neuropsychological Battery and the Minimal Assessment of Cognitive Function in MS. *Mult. Scler. J.* 15 (9), 1077–1084.
- Taulu, S., Simola, J., Kajola, M., 2005. Applications of the Signal Space Separation Method. *IEEE Trans. signal Process.* 53 (9), 3359–3372.
- Tewarie, P., Schoonheim, M.M., Stam, C.J., van der Meer, M.L., van Dijk, B.W., Barkhof, F., Polman, C.H., Hillebrand, A., Barnes, G.R., 2013. Cognitive and clinical dysfunction, altered MEG resting-state networks and thalamic atrophy in multiple sclerosis. *PLoS One*. 8 (7), e69318. <https://doi.org/10.1371/journal.pone.0069318>.
- Van der Meer, M.L., Tewarie, P., Schoonheim, M.M., et al., 2013. Cognition in MS correlates with resting-state oscillatory brain activity: An explorative MEG source-space study. *NeuroImage. Clin.* 2, 727–734.
- Van Schependom, J., Sjögård, M., Vidaurre, D., et al., 2019. Altered transient brain dynamics in multiple sclerosis: Treatment or pathology? *Hum. Brain Mapp.* 40 (16), 4789–4800. <https://doi.org/10.1002/hbm.24737>.
- Van Schependom, J., D'hooghe, M.B., Cleynhens, K., et al., 2014. Reduced information processing speed as primum movens of cognitive decline in Multiple Sclerosis. *Mult. Scler.* 21 (1), 83–91.
- Van, J., Schependom, D'hooghe, M.B., Cleynhens, K., et al., 2014. The Symbol Digit Modalities Test as sentinel test for cognitive impairment in MS. *Eur. J. Neurol.* 21 (9).
- Vidaurre, D., Hunt, L.T., Quinn, A.J., et al., 2018. Spontaneous cortical activity transiently organises into frequency specific phase-coupling networks. *Nat. Commun.* 9 (1), 2987.
- Vidaurre, D., Quinn, A.J., Baker, A.P., Dupret, D., Tejero-Cantero, A., Woolrich, M.W., 2016. Spectrally resolved fast transient brain states in electrophysiological data. *Neuroimage* 126, 81–95.
- Woolrich, M., Hunt, L., Groves, A., Barnes, G., 2011. MEG beamforming using Bayesian PCA for adaptive data covariance matrix regularization. *Neuroimage*. 57 (4), 1466–1479.
- Zhang, B., Hua, R., Qing, Z., Ni, L., Zhang, X., Zhao, H., Liu, R., Lu, J., Wu, S., Xu, Y., Zhu, B., Wan, S., Sun, Y., 2019. Abnormal brain functional connectivity coupled with hypoperfusion measured by Resting-State fMRI: An additional contributing factor for cognitive impairment in patients with Alzheimer's disease. *Psychiatry Res. - Neuroimaging*. 289, 18–25.